JJMIE

Volume 8 Number 5, October 2014
ISSN 1995-6665
Pages 333 - 342

Jordan Journal of Mechanical and Industrial Engineering

PSO-Based Neural Network Prediction and its Utilization in GMAW Process

Pathiyasseril Sreeraj [a *], Thangavel Kannan [b], Subhasis Maji [c]

[a] Department of Mechanical Engineering, Valia Koonambaikulathamma College of Engineering Technology, Kerala, 692574 India

[b] Principal, SVS College of Engineering,Coimbatore,Tamilnadu,642109 India.

[c] Professor, Department of Mechanical Engineering IGNOU, Delhi,110068, India

Received 31 Jan 2013 Accepted 25 Sep 2014

Abstract

This paper presents a Particle Swarm Optimization (PSO) technique in training an Artificial Neural Network (ANN) which is used for predicting Gas Metal Arc Welding (GMAW) process parameters for a given input set of welding parameters. Experiments were conducted according to central composite rotatable design with full replication technique and results are used to develop a multiple regression model. Multiple set of data from multiple regression are utilised to train the intelligent network. The trained network is used to predict the weld bead geometry. The welding parameters welding current, welding speed, contact tip to distance, welding gun angle and pinch are predicted with consideration of performance of bead width, penetration, reinforcement and dilution. Instead of training with conventional back propagation algorithm a new concept of training with PSO algorithm is used in this paper. The proposed ANN-PSO model developed using MATLAB function is found to be flexible, speedy and accurate than conventional ANN system.

Keywords: *: GMAW, Weld Bead Geometry, Multiple Regression, ANN, PSO.*

1. Introduction

Prediction of bead geometry in welding plays an important role in improving the quality of weld. The quality of a weld depends on mechanical properties of the weld metal which in turn depends on metallurgical characteristics and chemical composition of the weld. The mechanical and metallurgical feature of weld depends on bead geometry which is directly related to welding process parameters. In other words quality of weld depends on in process parameters [1, 2]. GMA welding is a multi-objective and multifactor metal fabrication technique. The process parameters have a direct influence on bead geometry. Much effort has been done for predicting the bead geometry using artificial neural network. Due to their excellent ability in mapping, generalisation, self-organisation and self-learning ANN became a powerful tool. Particle Swarm Optimization (PSO) is an evolutionary computational technique originated from the behaviour of bird flocking and fish schooling. In this paper a new method of training, instead of Back Propagation (BP) training, for ANN with PSO training is used.

Figure 1 shows the clad bead geometry. Mechanical strength of clad metal is highly influenced by the composition of metal but also by clad bead shape [2, 3]. This is an indication of bead geometry. It mainly depends on wire feed rate, welding speed, arc voltage etc. Therefore, it is necessary to study the relationship between in-process parameters and bead parameters to study clad bead geometry in which A and B represents area of reinforcement and area of penetration respectively. This paper highlights the study carried out to develop mathematical, ANN and ANN-PSO models to predict clad bead geometry in stainless steel cladding deposited by GMAW.

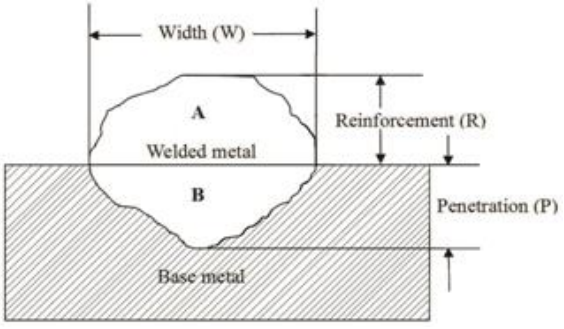

Percentage dilution (D) = [B/ (A+B)] X 100

Figure 1. Clad bead geometry

* Corresponding author. e-mail: pathiyasseril@yahoo.com.

  - Volume 8, Number 5 (ISSN 1995-6665)

2. Experimentation

The following machines and consumables were used for the purpose of conducting experiment:

1. A constant current gas metal arc welding machine (Invrtee V 350 – PRO advanced processor with 5 – 425 amps output range)
2. Welding manipulator
3. Wire feeder (LF – 74 Model)
4. Filler material Stainless Steel wire of 1.2mm diameter (ER – 308 L).
5. Gas cylinder containing a mixture of 98% argon and 2% of oxygen.
6. Mild steel plate (grade IS – 2062)

Test plates of size 300 x 200 x 20mm were cut from mild steel plate of grade IS – 2062 and one of the surfaces is cleaned to remove oxide and dirt before cladding. ER-308 L stainless steel wire of 1.2mm diameter was used for depositing the clad beads through the feeder. Argon gas at a constant flow rate of 16 litres per minute was used for shielding. The properties of base metal and filler wire are shown in Table 1. The important and most difficult parameter found from trial run is wire feed rate. The wire feed rate is proportional to current. Wire feed rate must be greater than critical wire feed rate to achieve pulsed metal transfer. The relationship found from trial run is shown in equation (1). The formula derived is shown in Figure 2:

$$\text{Wire feed rate} = 0.96742857 * \text{current} + 79.1 \quad (1)$$

The selection of the welding electrode wire based on the matching the mechanical properties and physical characteristics of the base metal, weld size and existing electrode inventory [4]. A candidate material for cladding which has excellent corrosion resistance and weld ability is stainless steel. These have chloride stress corrosion cracking resistance and strength significantly greater than other materials. These have good surface appearance, good radiographic standard quality and minimum electrode wastage.

Table 1. Chemical Composition of Base Metal and Filler Wire

	Elements, Weight %								
Materials	C	SI	Mn	P	S	Al	Cr	Mo	Ni
IS 2062	0.150	0.160	0.870	0.015	0.016	0.031	-	-	-
ER308L	0.03	0.57	1.76	0.021	1.008	-	19.52	0.75	10.02

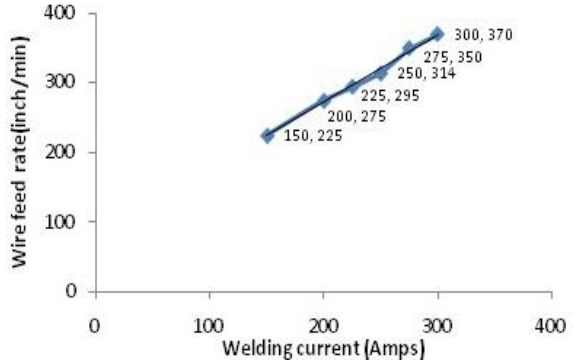

Figure 2. Relationship between Current and Wire Feed Rate

3. Plan of Investigation

The research work is carried out in the following steps [5,6] .Identification of factors ,finding the limit of process variables, development of design matrix, conducting experiments as per design matrix, recording responses, development of mathematical models, checking adequacy of developed models, and predicting the parameters using ANN, and using ANN-PSO parameters predicted**.**

3.1. Identification of Factors and Responses

The basic difference between welding and cladding is the percentage of dilution. The properties of cladding are significantly influenced by the dilution obtained. Hence, the control of the dilution is important in cladding where a low dilution is highly desirable. When dilution is quite low, the final deposit composition will be closer to that of the filler material and, hence, the corrosion resistant properties of cladding will be greatly improved. The chosen factors have been selected on the basis of getting minimal dilution and optimal clad bead geometry [1]. These are: wire feed rate (W), welding speed (S), and welding gun angle (T), contact tip. The following independently controllable process parameters were found to be affecting output parameters distance (N) and pinch (Ac). The responses chosen were clad bead width (W), height of reinforcement (R), Depth of Penetration (P), and percentage of dilution (D). The responses were chosen based on the impact of parameters on the final composite model.

3.2. Finding the Limits of Process Variables

Working ranges of all the selected factors are fixed by conducting a trial run. This was carried out by varying one of factors while keeping the rest as constant values. The working range of each process parameters was decided upon by inspecting the bead for smooth appearance without any visible defects. The upper limit of the given factor was coded as -2. The coded values of intermediate values were calculated using the equation (2):

$$\text{Xi} = \frac{2[2X - (X\,\text{max} + X\,\text{mi})]}{(X\,\text{max} - X\,\text{min})]} \quad (2)$$

Where X_i is the required coded value of parameter X is any value of parameter from Xmin – X_{max}. X_{min} is the lower limit of parameters and X_{max} is the upper limit parameters [7].

The chosen level of the parameters with their units and notation are given in Table 2:

3.3. Development of Design Matrix

The design matrix chosen to conduct the experiments was a central composite rotatable design. The design matrix comprises full replication of 2^5(= 32), and factorial designs. All welding parameters in the intermediate levels (o) constitute the central points and a combination of each welding parameter at either highest value (+2) or lowest (-2) with other parameters of intermediate levels (0) that constitute star points. 32 experimental trails were conducted, making the estimation of linear quadratic and two way interactive effects of process parameters on clad geometry [8,9].

3.4. Conducting Experiments as per Design Matrix

In this work, 32 experimental runs were allowed for the estimation of linear quadratic and two-way interactive effects corresponding to each treatment combination of parameters on bead geometry at random as shown Table 3. At each run, settings for all parameters were disturbed and reset for the next deposit. Figure 3 shows the GMAW circuit diagram. This is very essential for introducing variability caused by errors in the experimental set up. The experiments were conducted at SVS College of Engineering, Coimbatore, 642109, India.

3.5. Recording of Responses

For measuring the clad bead geometry, the transverse section of each weld overlays was cut using a band saw of mid length. Position of the weld and end faces were machined and grinded. The specimen and faces were polished and etched using a 5% nital solution to display bead dimensions. The clad bead profiles were traced using a reflective type optical profile projector at a magnification of X10, in M/s Roots Industries Ltd. Coimbatore. Then, the bead dimensions, such as depth of penetration height of reinforcement and clad bead width, were measured [10, 11]. The profiles traced using AUTO CAD software. This is shown in Figure 4. This represents the profile of the specimen (front side). The cladded specimen is shown in Figure 5. The measured clad bead dimensions and percentage of dilution are shown in Table 4.

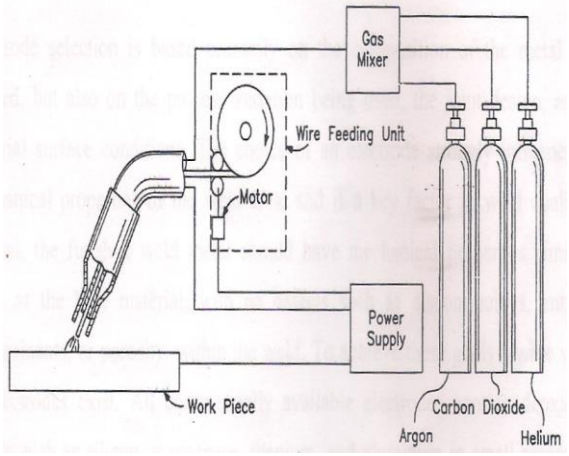

Figure 3. GMAW Circuit Diagram

Table 2. Welding Parameters and their Levels

Parameters	Factor Levels						
	Unit	Notation	-2	-1	0	1	2
Welding Current	A	1	200	225	250	275	300
Welding Speed	mm/min	S	150	158	166	174	182
Contact tip to work distance	mm	N	10	14	18	22	26
Welding gun Angle	Degree	T	70	80	90	100	110
Pinch	-	Ac	-10	-5	0	5	10

Table 3. Design Matrix

Trial Number	Design Matrix				
	I	S	N	T	Ac
1	-1	-1	-1	-1	1
2	1	-1	-1	-1	-1
3	-1	1	-1	-1	-1
4	1	1	-1	-1	1
5	-1	-1	1	-1	-1
6	1	-1	1	-1	1
7	-1	1	1	-1	1
8	1	1	1	-1	-1
9	-1	-1	-1	1	-1
10	1	-1	-1	1	1
11	-1	1	-1	1	1
12	1	1	-1	1	-1
13	-1	-1	1	1	1
14	1	-1	1	1	-1
15	-1	1	1	1	-1
16	1	1	1	1	1
17	-2	0	0	0	0
18	2	0	0	0	0
19	0	-2	0	0	0
20	0	2	0	0	0
21	0	0	-2	0	0
22	0	0	2	0	0
23	0	0	0	-2	0
24	0	0	0	2	0
25	0	0	0	0	-2
26	0	0	0	0	2
27	0	0	0	0	0
28	0	0	0	0	0
29	0	0	0	0	0
30	0	0	0	0	0
31	0	0	0	0	0
32	0	0	0	0	0

I - Welding current; S - Welding speed; N - Contact tip to work distance; T - Welding gun angle; Ac – Pinch

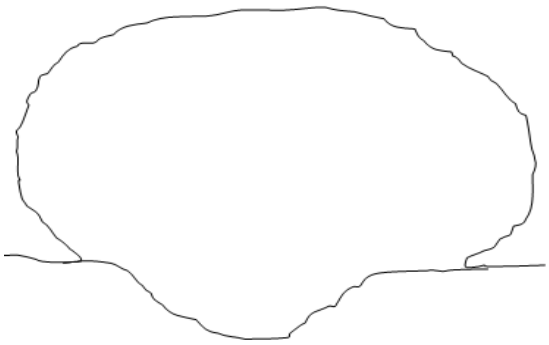

Figure 4. Traced Profile of bead geometry

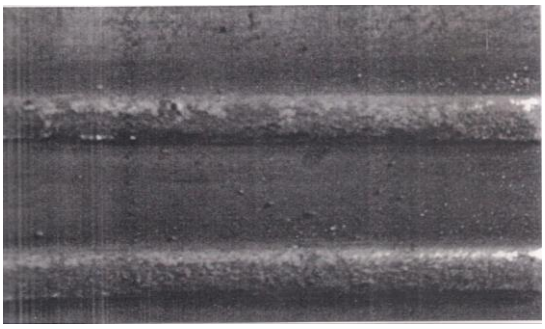

Figure 5. cladded specimen

Table 4. Design Matrix and Observed Values of Clad Bead Geometry

Trial No.	Design Matrix					Bead Parameters			
	I	S	N	T	Ac	W (mm)	P (mm)	R (mm)	D (%)
1	-1	-1	-1	-1	1	6.9743	1.67345	6.0262	10.72091
2	1	-1	-1	-1	-1	7.6549	1.9715	5.88735	12.16746
3	-1	1	-1	-1	-1	6.3456	1.6986	5.4519	12.74552
4	1	1	-1	-1	1	7.7635	1.739615	6.0684	10.61078
5	-1	-1	1	-1	-1	7.2683	2.443	5.72055	16.67303
6	1	-1	1	-1	1	9.4383	2.4905	5.9169	15.96692
7	-1	1	1	-1	-1	6.0823	2.4672	5.49205	16.5894
8	1	1	1	-1	-1	8.4666	2.07365	5.9467	14.98494
9	-1	-1	-1	1	-1	6.3029	1.5809	5.9059	10.2749
10	1	-1	-1	1	1	7.0136	1.5662	5.9833	9.707297
11	-1	1	-1	1	1	6.2956	1.58605	5.5105	11.11693
12	1	1	-1	1	-1	7.741	1.8466	5.8752	11.4273
13	-1	-1	1	1	1	7.3231	2.16475	5.72095	15.29097
14	1	-1	1	1	-1	9.6171	2.69495	6.37445	18.54077
15	-1	1	1	1	-1	6.6335	2.3089	5.554	17.23138
16	1	1	1	1	1	10.514	2.7298	5.4645	20.8755
17	-2	0	0	0	0	6.5557	1.99045	5.80585	13.65762
18	2	0	0	0	0	7.4772	2.5737	6.65505	15.74121
19	0	-2	0	0	0	7.5886	2.50455	6.4069	15.77816
20	0	2	0	0	0	7.5014	2.1842	5.6782	16.82349
21	0	0	-2	0	0	6.1421	1.3752	6.0976	8.941799
22	0	0	2	0	0	8.5647	3.18536	5.63655	22.94721
23	0	0	0	-2	0	7.9575	2.2018	5.8281	15.74941
24	0	0	0	2	0	7.7085	1.85885	6.07515	13.27285
25	0	0	0	0	-2	7.8365	2.3577	5.74915	16.63287
26	0	0	0	0	2	8.2082	2.3658	5.99005	16.38043
27	0	0	0	0	0	7.9371	2.1362	6.0153	15.18374
28	0	0	0	0	0	8.4371	2.17145	5.69895	14.82758
29	0	0	0	0	0	9.323	3.1425	5.57595	22.8432
30	0	0	0	0	0	9.2205	3.2872	5.61485	23.6334
31	0	0	0	0	0	10.059	2.86605	5.62095	21.55264
32	0	0	0	0	0	8.9953	2.72068	5.7052	19.60811

W-Width; R - Reinforcement W - Width; P - Penetration; D - Dilution %

3.6. Development of Mathematical Models

The response function representing any of the clad bead geometry can be expressed as [12, 13]:

$$Y = f(A, B, C, D, E) \quad (3)$$

Where,
Y = Response variable
A = Welding current (I) in amps
B = Welding speed (S) in mm/min
C = Contact tip to Work distance (N) in mm
D = Welding gun angle (T) in degrees
E = Pinch (Ac)

The second order surface response model equals can be expressed as below:

$$Y = \beta_0 + \sum_{i=0}^{5} \beta_i X_i + \sum_{i=0}^{5} \beta_n x_i^2 + \sum_{i=0}^{5} X_{ij} X_j \quad (4)$$

$$Y = \beta_0 + \beta_1 A + \beta_2 B + \beta_3 C + \beta_4 D + \beta_5 E + \beta_{11} A^2 + \beta_{22} B^2 + \beta_{33} C^2 + \beta_{44} D^2 + \beta_{55} E^2 + \beta_{12} AB + \beta_{13} AC + \beta_{14} AD + \beta_{15} AE + \beta_{23} BC + \beta_{24} BD + \beta_{25} BE + \beta_{34} CD + \beta_{35} CE + \beta_{45} DE$$

Where, β_0 is the free term of the regression equation, the coefficient β_1, β_2, β_3, β_4 and β_5 is are linear terms, the coefficients β_{11}, β_{22}, β_{33}, β_{44} and β_{55} quadratic terms, and the coefficients β_{12}, β_{13}, β_{14}, β_{15}, etc are the interaction terms. The coefficients were calculated by using Quality America six sigma software (DOE – PC IV). After determining the coefficients, the mathematical models were developed. The developed mathematical models are given as follows:

$$\beta_0 = 0 \cdot 166338((\Sigma X_0 Y) + 0.05679(\Sigma \Sigma X_{ii} Y)) \quad (5)$$

$$\beta_i = 0.166338(\Sigma X_i Y) \quad (6)$$

$$\beta_{ii} = 0.0625((\Sigma X_{ii} Y) + 0.06889(\Sigma \Sigma X_{ii} Y) - 0.056791(\Sigma \Sigma X_0 Y)) \quad (7)$$

$$\beta_{ij} = 0.125(\Sigma X_{ij} Y) \quad (8)$$

Clad Bead Width (W), mm = 8.923 + 0.701A + 0.388B + 0.587C + 0.040D + 0.088E – 0.423A2 – 0.291B2 – 0.338C2 – 0.219D2 – 0.171E2 + 0.205AB + 0.405AC + 0.105AD + 0.070AE–0.134BC+0.225BD+0.098BE+ 0.26CD+0.086CE+0.012DE (9)

Depth of Penetration (P), mm = 2.735 + 0.098A – 0.032B + 0.389C – 0.032D – 0.008E – $0.124A^2$ – $0.109B^2$ – $0.125C^2$ – $0.187D^2$ – $0.104E^2$ – 0.33AB + 0.001 AC + 0.075AD + 0.005 AE–0.018BC+ 0.066BD+ 0.087BE + 0.058CD + 0.054CE – 0.036DE (10)

Height of Reinforcement (R), mm = 5.752 + 0.160A – 0.151B – 0.060C + 0.016D – 0.002E + $0.084A^2$ + $0.037B^2$ – $0.0006C^2$ + $0.015D^2$ – $0.006E^2$ + 0.035AB + 0.018AC – 0.008AD – 0.048AE– 0.024BC – 0.062BD –0.003BE + 0.012CD – 0.092CE–0.095DE (11)

Percentage Dilution (D), % = 19.705 + 0.325A + 0.347B + 3.141C – 0.039D – 0.153E – $1.324A^2$ – $0.923B^2$ – $1.012C^2$ – $1.371D^2$ – $0.872E^2$ – 0.200AB + 0.346 AC + 0.602 AD + 0.203AE + 0.011BC + 0.465BD + 0.548BE + 0.715CD + 0.360CE+0.137DE (12)

Co-efficient of the above polynomial equation where calculated by regression as given by equations (5) to (8)

3.7. Checking the Adequacy of the Developed Models

Analysis of variance (ANOVA) technique was used to test the adequacy of the model. As per this technique, if the F – ratio values of the developed models do not exceed the standard tabulated values for a desired level of confidence (95%) and the calculated R – ratio values of the developed model exceed the standard values for a desired level of confidence (95%) then the models are said to be adequate within the confidence limit [14]. These conditions were satisfied for the developed models. The values are shown in Table 5:

Table 5. Analysis of variance for Testing Adequacy of the Model

Parameter	1st Order terms		2nd order terms		Lack of fit		Error terms		F-ratio	R-ratio	Whether model is adequate
	SS	DF	SS	DF	SS	DF	SS	DF			
W	36.889	20	6.233	11	3.51 3	6	2.721	5	1.076	3.390	Adequate
P	7.810	20	0.404	11	0.142	6	0.261	5	0.454	7.472	Adequate
R	1.921	20	0.572	11	0.444	6	0.128	5	2.885	3.747	Adequate
D	506.074	20	21.739	11	6.289	6	15.45	5	0.339	8.189	Adequate

SS - Sum of squares; DF - Degree of freedom; F Ratio (6, 5, 0.5) = 3.40451; R Ratio (20, 5, 0.05) = 3.20665

4. Artificial Neural Network

Artificial neural network models are generally comprised of three independent layers: input, hidden, and output. Each layer consists of several processing neurons. Each neuron in a layer operates in logical similarity. Information is transmitted from one layer to others in serial operations. The neurons in the input layer include the input values. Each neuron in the hidden layer processes the inputs into the neuron outputs. The pattern of hidden layers to be applied in the modelling can be either multiple layers or a single layer. The most widely used training algorithm for neural networks is the back-propagation algorithm [15, 16].

The MLP is one of artificial neural networks that are extensively used to solve a number of different problems, including pattern recognition and interpolation. Each layer is composed of neurons which are interconnected with each other in a previous layer by weights. In each neuron, a specific mathematical function called the activation function accepts a weighed sum of the outputs from a previous layer as the function's input, and generates the function's output. In the experiment, the hyperbolic tangent sigmoid transfer function [17] is used as the activation function. It is defined by:

$$f(s) = \frac{1-e^{-2s}}{1-e^{-2s}} \tag{13}$$

Where $S = \sum_{i-0}^{n} wixi + b$ in which w_i are weights, x_i are inputs of neuron, b is bias and n is the number of variables.

The MLP is trained by using the Levenberg-Marquardt technique. This technique is more powerful than the conventional gradient descent technique.

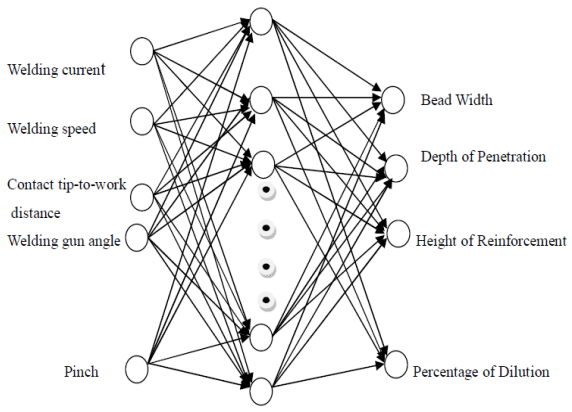

Figure 6. Neural Network Architecture

MAT LAB 7 was used for training the network for the prediction of clad bead geometry. Statistical mathematical model was used compare results produced by the work. For normalizing the data the goal is to examine the statistical distribution of values of each net input and outputs are roughly uniform in addition the value should scaled to match range of input neurons [18]. This is basically range 0 to 1 in practice it is found to between 01 and 9. In this paper, data bases are normalized using the Equation (9):

$$X_{norm} = 0.1 + \frac{(X - X_{min})}{1.25(X_{max} - (X_{min})} \tag{14}$$

X_{norm} = Normalized value between 0 and 1
X = Value to be normalized
X_{min} = Minimum value in the data set range the particular data set rage which is to be normalized.
X_{max} = Maximum value in the particular data set range which is to be normalized.

The accuracy of prediction may be decreased with the increase in the number of neurons in the hidden layer in other words increase in number of neurons could not directly improve the capability of function approximation of network. In this study, five welding process parameters were employed as input to the network. The Levenberg-Marquardt approximation algorithm was found to be the best fit for application because it can reduce the MSE to a significantly small value and can provide better accuracy of prediction. So, neural network model with feed forward back propagation algorithm and Levenberg-Marquardt approximation algorithm was trained with data collected for the experiment. Error was calculated using equation (10):

$$\text{Error} = \frac{(Actual \text{ value - Predicted value}) \text{ X } 100}{\text{Predicted value}} \tag{15}$$

The difficulty using the regression equation is the possibility of over fitting the data. To avoid this the experimental data is divided in to two sets, one training set and other test data set .The ANN model is created using only training data the other test data is used to check the behaviour the ANN model created. All variables are normalized using the equation (9).The data was randomized and portioned in to two one training and other test data.

$$y = \sum_i w_{ij} h_i + \theta \tag{16}$$

$$h_i = \tan h(\Sigma_j w_{ij} x_j + \theta_i) \tag{17}$$

The Neural Network general form can be defined as a model shown above y representing the output variables and x_j the set of inputs, shown in equations [19, 20]. The subscript $_i$ represents the hidden units shown in Figure 6 and θ represents the bias and w_j represents the weights. The equation above defines the function giving output as a function of input.

In this work, the number of input neurons is five and output neurons are four. It is necessary to find the number of hidden layers and number of neurons in the hidden layer. From Figure 7, it is found that twelve neurons give minimum error. So, a structure of 5-12-4 is created for the prediction of data. The data for prediction are taken from Table 4. First eleven data are used for testing and the next seventeen data are used for training. This is shown in Tables 7 and 8.

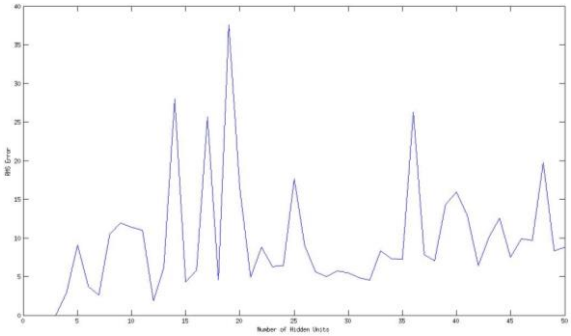

Figure7. comparisons between number of hidden units and Error

Table 6. Comparison of actual and predicted values of the clad bead parameters using neural network data (training)

Trial NO	Actual Bead Parameters				Predicted Bead Parameters				Error			
	W (mm)	P (mm)	R (mm)	D (%)	W (mm)	P (mm)	R (mm)	D (%)	W (mm)	P (mm)	R (mm)	D (%)
1	7.741	1.8466	5.8752	11.4273	7.335	2.0986	6.0792	10.8222	0.406	-0.252	-0.204	0.6051
2	7.3231	2.16475	5.72095	15.29097	6.8214	2.0617	5.6946	14.9379	0.5017	0.10305	0.02635	0.35307
3	9.6171	2.69495	6.37445	18.54077	9.3713	2.8982	6.4084	17.4578	0.2458	0.20325	-0.0339	1.08297
4	6.6335	2.3089	5.554	17.23138	7.4306	2.2927	5.6232	15.7908	-0.7971	0.0162	-0.0692	1.44058
5	10.514	2.7298	5.4645	20.8755	7.8991	2.5154	5.8078	18.0664	2.6149	0.2144	-0.3433	2.8091
6	6.5557	1.99045	5.80585	13.65762	6.5761	1.9158	5.7867	14.2039	-0.0204	0.07465	0.01915	-0.5462
7	7.4772	2.5737	6.65505	15.74121	7.393	2.7191	6.7112	14.7525	0.0842	-0.1454	-0.0561	0.98871
8	7.5886	2.50455	6.4069	15.77816	7.5943	2.4317	6.3834	15.9881	-0.0057	0.07285	0.0235	-0.2099
9	7.5014	2.1842	5.6782	16.82349	7.4652	2.2814	5.7674	16.5744	0.0362	-0.0972	-0.0892	0.24909
10	6.1421	1.3752	6.0976	8.941799	5.6583	1.44	6.2054	9.3753	0.4838	-0.0648	-0.1078	-0.4335
11	8.5647	3.18536	5.63655	22.94721	9.9724	2.962	5.5227	18.9566	-1.4077	0.22336	0.11385	3.99061
12	7.9575	2.2018	5.8281	15.74941	9.0693	2.6919	6.2337	17.5548	-1.1118	-0.4901	-0.4056	-1.8053
13	7.7085	1.85885	6.07515	13.27285	6.7699	1.7807	6.109	12.8584	0.9386	0.07815	-0.0338	0.41445
14	7.8365	2.3577	5.74915	16.63287	8.5364	2.9431	6.6735	15.9653	-0.6999	-0.5854	-0.9243	0.66757
15	8.2082	2.3658	5.99005	16.38043	8.0083	2.371	6.0186	16.3701	0.1999	-0.0052	-0.0285	0.01033
16	7.9371	2.1362	6.0153	15.18374	7.9441	2.1197	6.01	15.3735	-0.007	0.0165	0.0053	-0.1897
17	8.4731	2.17145	5.69895	14.82758	8.6735	2.5165	5.4985	15.2875	-0.2001	-0.3450	0.2031	-0.4599

Table 7. Comparison of actual and predicted values of the clad bead parameters using neural network data (test)

Trial No	Actual Bead Parameters				Predicted Bead Parameters				Error			
	W (mm)	P (mm)	R (mm)	D (%)	W (mm)	P (mm)	R (mm)	D (%)	W (mm)	P (mm)	R (mm)	D (%)
1	6.9743	1.6735	6.0262	10.721	6.1945	1.85	5.9611	12.367	0.7798	-0.177	0.0651	-1.646
2	7.6549	1.9715	5.8873	12.167	7.1815	2.1507	6.5553	10.268	0.4734	-0.179	-0.668	1.899
3	6.3456	1.6986	5.4519	12.746	7.4954	1.5339	5.4923	9.3808	-1.15	0.1647	-0.04	3.3652
4	7.7635	1.7396	6.0684	10.611	6.4936	1.854	6.5573	9.4799	1.2699	-0.114	-0.489	1.1311
5	7.2683	2.443	5.7206	16.673	7.3354	2.6576	5.5657	19.104	-0.067	-0.215	0.1549	-2.431
6	9.4383	2.4905	5.9169	15.967	7.6066	2.1045	6.4342	18.49	1.8317	0.386	-0.517	-2.523
7	6.0823	2.4672	5.492	16.589	8.0417	2.1722	5.5126	16.874	-1.959	0.295	-0.021	-0.285
8	8.4666	2.0737	5.9467	14.985	8.3236	2.2349	5.9031	16.972	0.143	-0.161	0.0436	-1.987
9	6.3029	1.5809	5.9059	10.275	8.2381	1.7955	5.6022	11.219	-1.935	-0.215	0.3037	-0.944
10	7.0136	1.5662	5.9833	9.7073	7.5899	2.4579	6.542	13.415	-0.576	-0.892	-0.559	-3.708
11	6.2956	1.586	5.5105	11.117	7.7318	1.7647	5.8676	10.71	-1.436	-0.179	-0.357	0.407

5. PSO algorithm

The particle swarm optimization algorithm gives a solution much similar to problems such as genetic algorithms. In PSO, a point in the problem space is called a particle, which is initialized with a random position and search velocity [21, 22]. Each particle flies through the problem space and keeps track of its positions and its fitness. Where the latter means the best solution achieved. Its position and velocity are adjusted by its fitness to the environment. Given that a swarm consists of *m* particles in a D-dimensional problem space, the position and velocity of the *i*th particle is presented as:

$Si = (Si_1, Si_2, \ldots, Si_D)$, i=1,2…..m,

$vi = (vi_1, vi_2, \ldots vi_D)$

The best position of a particle is denoted by P_{best}, $pi = (pi_1, pi_2 \ldots\ldots pi_3)$. Treating the swarm population as a

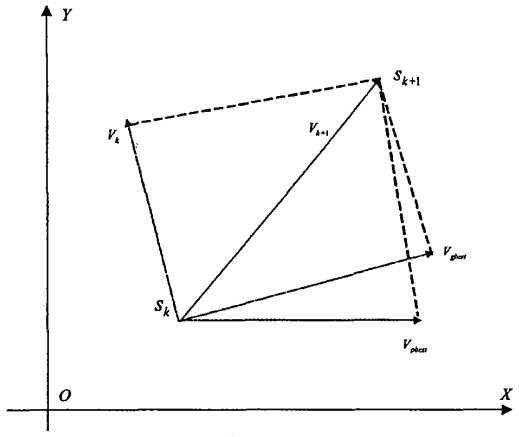

Figure 8. The illustration of searching in a two – dimensional space.

Whole, the best position of the best positions of all particles is denoted by G_{best} in which $p_g=(p_{g1},p_{g2},\ldots\ldots p_{g3})$.

The PSO algorithm is formulated as [12]:

$$v_{id}^{k+1} = w_{id}^{k} + c_1 \text{ran}\, d_1(Pbest - s_{id}^{k}) + c_2 \text{ran}\, d_2(g_{best} - s_{id}^{k}) \quad (18)$$

$$S_{Id}^{k+1} = s_{id}^{k} + v_{id}^{k+1}, \; i = 1, 2, \ldots, m, \; d = 1, 2, \ldots, D \quad (19)$$

where, v_{id}^{k} is the velocity of the *i*th particle at the *k*th iteration, *w* the inertia weight, c_j the accelerating factor, rand the random in a range [0, 1] and s_{id}^{k} is the current position of the *i*th particle.

Figure 8 illustrates the search process of a particle in a two-dimensional space, where S^k is the current position, S^{k+1} the search position next to the current position, v^k the velocity at the current position, v^{k+1} the velocity at the next position, p_{best} the best velocity based on the v_{best} and u_p is the velocity based on G_{best}

To ensure the convergence of the search, a constriction factor is introduced into the standard PSO algorithm. Eq. (18) is converted into:

From Eq. (20), *k* is constricted by c_1 and c_2. Due to *k*, there is no need of the maximum search velocity V_{max} and the search convergence is ensured mathematically. In other words, the vibration amplitude of the particle decreases when it is near to the best position. Obviously, the constriction factor in the PSO algorithm can produce the solution better than that of the standard PSO [21, 22].

6. Neural Network Training with PSO and Comparison

Instead of back propagation algorithm (BP) ANN is trained with PSO. The predicted results are shown in Table 8. Figure 9 shows convergence comparison.

$$v_{id}^{k+1} = k[v_{id}^{k} + c_1 \text{ran}\, d_1(Pbest - s_{id}^{k}) + c_2 \text{ran}\, d_2(g_{best} - s_{id}^{k})] \quad (20)$$

$$k = \frac{2}{|2 - \varphi - \sqrt{\varphi^2 - 4\varphi}|} \qquad \text{Where } \varphi = c_1 + c_2 \varphi > 4\varphi. \quad (21)$$

Table 8. Comparison of actual and predicted data using ANN-PSO (Test)

Trial No	Actual Bead Parameters				Predicted Bead Parameters				Error			
	W (mm)	P (mm)	R (mm)	D (%)	W (mm)	P (mm)	R (mm)	D (%)	W (mm)	P (mm)	R (mm)	D (%)
1	6.9743	1.6735	6.0262	10.721	6.7317	1.5807	6.5376	10.192	0.2426	0.0928	-0.4114	0.5290
2	7.6549	1.9715	5.8873	12.167	7.7314	1.5231	4.5848	12.628	-0.0765	0.4484	1.3025	-0.461
3	6.3456	1.6986	5.4519	12.746	6.7698	1.9721	5.6432	12.588	-0.4242	-0.2735	-0.0913	0.158
4	7.7635	1.7396	6.0684	10.611	7.2224	1.7116	6.8496	11.665	0.3482	0.0820	-0.7812	1.044
5	7.2683	2.443	5.7206	16.673	7.6165	2.8299	5.5489	16.052	-0.3482	-0.3799	0.1717	0.621
6	9.4383	2.4905	5.9169	15.967	9.4902	2.4324	5.4616	15.729	-0.0512	0.0581	0.4545	0.2382
7	6.0823	2.4672	5.492	16.589	6.9565	2.4565	5.9655	15.654	-0.8742	0.0101	0.4730	0.9390
8	8.4666	2.0737	5.9467	14.985	8.4301	2.0245	5.3226	15.666	0.0366	0.0492	0.6241	-0.6811
9	6.3029	1.5809	5.9059	10.275	4.6652	1.8028	5.1061	10.997	1.6377	-0.2219	0.7998	-0.7218
10	7.0136	1.5662	5.9833	9.7073	6.4065	1.4028	5.6872	9.4375	0.6071	0.1634	0.1871	0.2698
11	6.2956	1.586	5.5105	11.117	5.9413	1.7973	5.0204	11.570	0.3543	-0.2219	0.4901	-0.453

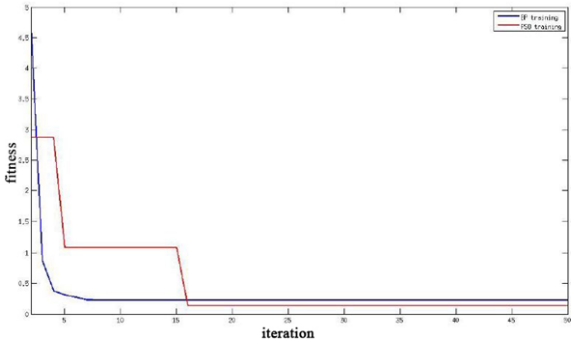

Figure 9. Convergence velocity comparison of the PSO and BP

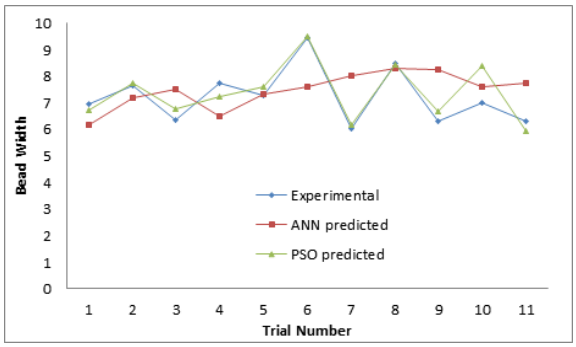

Figure 10. Comparison of ANN and ANN-PSO prediction in Bead Width

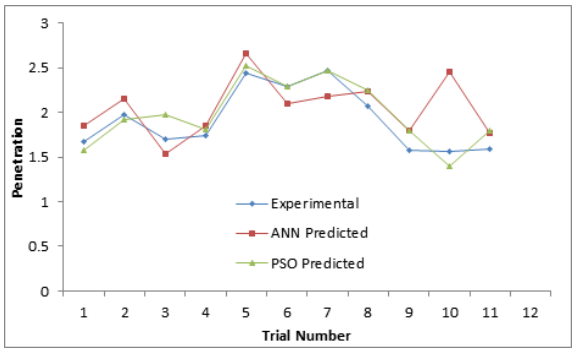

Figure 11. Comparison of ANN and ANN-PSO prediction in Penetration

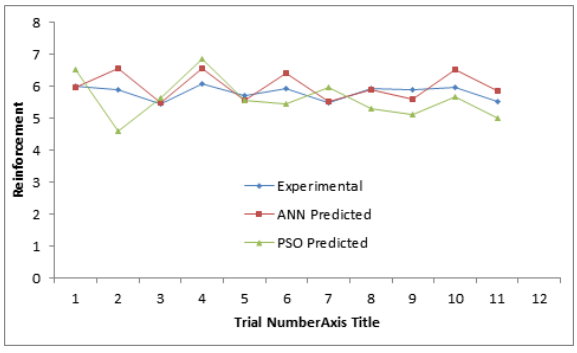

Figure 12. Comparison of ANN and ANN-PSO prediction in Reinforcement

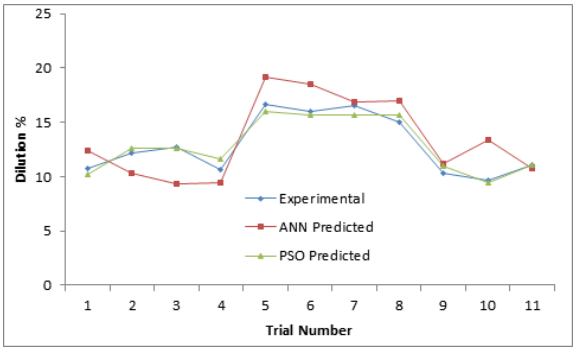

Figure 13. Comparison of ANN and ANN-PSO prediction in Percentage of Dilution

7. Results and Discussions

1. A five-level five-factor full factorial design matrix based on central composite rotatable design technique was used for the mathematical development of model to predict the clad bead geometry of austenitic stainless steel deposited by GMAW.
2. ANN tool, available in MATLAB 7 software, was efficiently employed for prediction of clad bead geometry.
3. In cladding by a welding process, clad bead geometry is very important for economising the material. This study effectively used ANN and ANN-PSO models to predict weld bead geometry.
4. In this study, two models Artificial Neural Network (ANN) and ANN-PSO system for prediction of bead geometry in GMAW welding process are studied and compared. It is proved that ANN-PSO model prediction is more efficient than neural network model. The comparison of prediction between ANN and ANN-PSO is shown through Figures 10-13.
5. The paper presents the adoption of a particle swarm optimization technique to train perceptrons in predicting the outcome of clad bead geometry. A key contribution of the presented work is the adoption of PSO-based training of prediction of bead geometry. The performance of the PSO-based multilayer ANN is bench marked with conventional BP base neural network. It is noted that the testing case of the PSO based network is able to give a successful prediction rate with less error. Moreover, the PSO-based perceptron exhibits much better and faster convergence performance in the training process as well as a better ability in the validation process than the conventional BP-based perceptron. It can be observed from Figure 9 that the PSO-based training is better than the conventional BP-based training. It can be concluded that the PSO-based perceptron performs better than the conventional BP-based perceptron.

8. Conclusions

Based on the above study, it can be observed that the developed model can be used to predict clad bead geometry within the applied limits of process parameters. In this study, ANN-PSO and ANN were used for predicting clad bead geometry. In the case of any cladding process, bead geometry plays an important role in determining the properties of the surface exposed to hostile environments and reducing cost of manufacturing. It is proved that PSO is faster and more accurate than ANN.

Instead of conventional back propagation algorithm used in the conventional artificial neural network training, a new method of PSO-based training of ANN is used in this study. It can be shown that error is less in PSO-based training and, thus, PSO-based training is more accurate, speedy and precise. While comparing the convergence of PSO and BP algorithms, PSO is better converged. Comparing reinforcement, penetration, bead width and dilution with conventional BP algorithm and new PSO training, it can be seen that the new method is acceptable and can be used in predicting the bead geometry.

Acknowledgement

The authors sincerely acknowledge the help and facilities extended to them by the department of mechanical engineering SVS college of Engineering, Coimbatore, India.

References

[1] T.Kannan, N. Murugan, "Effect of flux cored arc welding process parameters on duplex stainless steel clad quality". Journal of Material Processing Technology, Vol. 176 (2006) 230-239.

[2] T.Kannan, N.Murugan, B.N.Sreeharan, "Optimization of Flux cored arc welding process parameter using genetic and memetic algorithms". Journal of Manufacturing Science and Production, Vol. 13 (2013) No. 4, 239-250.

[3] Lijopaul, Somashekher, S. Hiremath, "Response surface modelling of micro holes in electro chemical discharge machining process". Procedia Engineering, Vol. 64 (2013), 1335-1404.

[4] K.Kalaiselvan, N. Murugan, " Optimization of friction stir welding process parameters for the welding of AL-B4C composite plates using generalised reduced gradient method". Procedia Engineering, Vol. 38 (2012) 49-55.

[5] Dawei Zhao, Yuanxun Wang, Suing Sheng, Zongguo Lin, " Multi-objective optimal design of small scale resistance spot welding process with principal component analysis and response surface methodology". Journal of Intelligent Manufacture, DOI10.1007/s 10845-013-0733-2, (2013).

[6] HariOm, Sunil Pandey, "Effect of heat input on dilution and heat affected zone in submerged arc welding process", Indian Academy of Sciences, Vol. 36 (2013) 1369-1391.

[7] Norasiah Muhammad, Yupiter HP Manurung, Mohammead Hafidzi, Sunhaji Kiyai Abas ,GhalibTham, EsaHaruman, "Optimization and modelling of spot welding parameters with simultaneous multiple response consideration using multi objective Taguchi method and RSM", Journal of Mechanical Science and Technology, Vol. 26 (2012) No. 8, 2365-2370.

[8] A.Pradeep, S. Muthumaran ,P.R. Dhanush ,T. Nakkeran , "A study on friction stir welding of low alloy steel by using a tool with conical pin". International Journal of Mechanical and Materials Engineering, Vol. 8 (2013) 132 - 137.

[9] T.Kannan, N. Murugn, "Prediction of ferrite number of duplex stainless steel clad metals using RSM". Welding Journal, Vol. 85 (2006) No. 5, 91-99.

[10] V.Gunaraj, N. Murugan, "Prediction and control of weld bead geometry and shape relationships in submerged arc welding of pipes". Journal of Material Processing Technology, Vol. 168 (2005) 478-487.

[11] I.S.Kim, K.J. Son, Y.SYang, P. K. D.V. Yaragada, (2003). "Sensitivity analysis for process parameters in GMA welding process using factorial design method". International Journal of Machine Tools and Manufacture, Vol. 43 (2003) 763-769.

[12] W.G Cochran, G.M Coxz, Experimental Design.3rd ed. New York: John Wiley & Sons ;(1987)

[13] Serdar Karaoglu, Abdullah Secgin, "Sensitivity analysis of submerged arc welding process parameters". Journal of Material Processing Technology, Vol. 202 (2008) 500-507.

[14] P.K.Ghosh, P.C. Gupta, V.K. Goyal, "Stainless steel cladding of structural steel plate using the pulsed current GMAW process". Welding journal,Vol. 77 (1998) No. 7, 307-314.

[15] V.Gunaraj, N. Murugan, " Prediction and comparison of the area of the heat effected zone for the bead on plate and bead on joint in SAW of pipes". Journal of Material Processing Technology, Vol. 95 (1999), 246-261.

[16] T.Kannan, Yoganath,"Effect of process parameters on clad bead geometry and shape relationships of stainless steel cladding deposited by GMAW". Int. Journal of Manufacturing Technology, Vol. 47 (2010) 1083-1095.

[17] S.N.Deepa, S.N Sivanandam, Introduction to Genetic Algorithms. Springer, ISBN-978-3-540-73989-4, Spin: 12053230.

[18] J. Edwin Raja Dhas, S. Kumaanan, "Optimization of process parameters of submerged arc welding using non-conventional techniques". Applied Soft Computing, Vol. 11 (2001) 5198-5204.

[19] P.K.Giridharan, N.Murugan, "Optimization of pulsed GTA welding process parameters for the welding of AISI 304 L stainless steel'. International Journal of Advanced Manufacturing Technology, Vol. 40 (2009) 478 - 489.

[20] k.Siva, N.Murugan, R.Logesh, "Optimisation of Weld Bead Geometry in Plasma Transferred Arc Hard faced Austenitic Stainless Steel Plates using Genetic Algorithm". International Journal of Advanced Manufacturing Technology, Vol. 4(2009) 24-30.

[21] Azlan Mohad Zain., Habibullah Haron, Safian Sharif, "Optimization of process parameters in abrasive water jet machining using integrated SA-GA". Applied Soft Computing, Vol. 11 (2011) 5350-5359.

[22] Jialin Zhou, Zhengcheng Duan, Yong Li, Jianchun Deng, Daoyuan Yu, "PSO based neural network optimization and its utilization in boring". Journal of Material Processing and Technology, Vol. 178 (2006) 19-23.